Hamedan University of Technology
Iranian Association of Electrical and Electronics Engineers

Sustainable Energy and Artificial Intelligence

Online ISSN: 3060-8015

Journal Homepage: www.enai.hut.ac.ir

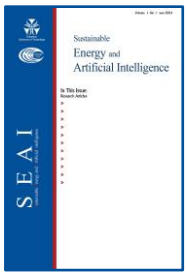

An Investigation of the Effects of Speckles Prepared Using Titanium Dioxide Powder and their Dimension on the Results of Digital Image Correlation (DIC) Method for Steel Specimen Elasticity Modulus Determination

Amir Masoud Hamidi Majd[1], Seyed Ebrahim Mousavi Torshizi[1], Javad Zare[2*]

[1] *Department of Mechanical and Energy Engineering, Shahid Beheshti University, Tehran, Iran*
[2] *Department of Mechanical Engineering, Shiraz University of Technology, Shiraz, Iran*
* *Corresponding Author: zare.mecheng@gmail.com*

Article Info

Article type:
Original Article

Article history:
Received 2025-08-16;
Revised 2025-10-22;
Accepted 2025-11-03.

How to cite this article:
Hamidi Majd, A. M, Mousavi Torshizi, S. E. and Zare, J. (2025). An Investigation of the Effects of Speckles Prepared Using Titanium Dioxide Powder and their Dimension on the Results of Digital Image Correlation (DIC) Method for Steel Specimen Elasticity Modulus Determination. *Sustainable Energy and Artificial Intelligence*, *2*(1), 15-24.
DOI: 10.61882/seai.2508-1033

Abstract

In recent years, Digital Image Correlation (DIC) method has gained attention as a non-contact technique for strain measurement. This study explores the potential of DIC to measure stress-strain behavior of a steel tensile test specimen and calculate the elastic modulus, comparing the results with analytical anticipations and resistive strain gauges measurements. For this purpose, a steel specimen with specified dimensions and material is prepared using white paint spray and subjected to tensile loading. The average absolute error of about 3.7% in strain measurements using resistive strain gauges compared to the analytical results demonstrates the capability of this method to accurately predict strain values. Although the DIC method can predict the linear stress-strain behavior, it shows a 45% error in calculating the elastic modulus compared to both resistive strain gauge measurements and analytical method predictions. To examine the effects of using titanium dioxide powder, preparing the specimen with this powder is recommended to enhance the brightness of the speckles and create sharper edges between the background and the painted speckles. This approach yields an elastic modulus prediction of 163 GPa compared to 183 GPa from the resistive strain gauge method (about a 10% difference), which is acceptable from an engineering perspective. Furthermore, increasing the speckle dimension reduces the prediction error of the elastic modulus to less than 5% compared to the both approaches. The results highlight the high potential of the DIC technique which could be so advantageous in predictive maintenance of energy infrastructure, or artificial intelligence (AI)/ data driven applications.

***Keywords*:** DIC, Resistive strain gauge, Wheatstone bridge, Ncorr, Elastic modulus.

1. Introduction

In recent years, the global shift towards sustainable energy systems and advanced infrastructure has led to an augmented demand for accurate, reliable, and non-invasive methodologies for evaluating the mechanical states of materials and structures. Energy-critical assets, including but not limited to wind turbine blades, boiler casings, pipelines, transmission towers, and smart grid components, are frequently subjected to intricate mechanical, thermal, and vibrational stresses that progressively compromise their structural integrity over time. The prompt identification of deformation, fatigue, or alterations in elastic properties is therefore of paramount importance, not solely to avert catastrophic failures and expensive downtimes, but also to facilitate efficient resource utilization,

extension of lifecycle, and the overarching sustainability of energy systems. Structural health monitoring paradigms are increasingly embracing predictive maintenance strategies, which leverage continuous or periodic sensing methodologies to foresee potential issues prior to their escalation into critical problems.

Conventional contact-based sensors, such as strain gauges, while exhibiting high precision, possess inherent limitations: they necessitate physical installation (which may prove challenging in harsh or inaccessible environments), may induce local alterations in material behavior, and are frequently impractical for comprehensive measurements across extensive or curved surfaces. These constraints catalyze a growing interest in non-contact, full-field measurement techniques, among which Digital Image Correlation (DIC) has emerged as a distinguished method [1].

DIC constitutes a non-contact optical methodology for quantifying displacement, strain, and geometrical attributes of materials and structures, and, with appropriate speckle pattern generation, imaging resolution, and calibration, can achieve precision comparable to or nearing that of contact sensors. This technique has witnessed an increasing application in the domains of structural health monitoring and maintenance of energy systems [2, 3].

Evaluating the structural integrity of wind turbine blades [4-11], identifying faults and conducting maintenance on solar panel systems [12, 13], performing inspections within the nuclear sector [14], and monitoring pipelines [15] represent merely a few instances of the broad applications of this method within energy-related sectors.

The integration of artificial intelligence (AI) and machine learning (ML) with DIC has opened new frontiers in experimental mechanics and structural health monitoring. Fundamental DIC methodologies depend on computationally demanding correlation algorithms to convert speckle images into displacement and strain fields; however, recent breakthroughs in deep learning have illustrated that neural networks can establish direct end-to-end mappings from speckle patterns to full-field deformation data, thus significantly expediting computational processes and enabling near real-time analysis. Deep DIC serves to diminish computational time while preserving accuracy [16].

Melching et al. [17] implemented machine learning techniques for accurate crack detection and preventative maintenance of components subjected to fatigue loading. Convolutional neural networks have been utilized to localize damage features, including the initiation and propagation of fatigue cracks, directly from DIC-derived strain maps, with interpretable ML methodologies such as Grad-CAM enhancing the elucidation of predictions in contexts critical to safety [18]. These advancements unequivocally illustrate the intrinsic relationship between image-based DIC and AI. DIC captures high-fidelity, full-field experimental data, while AI provides the requisite computational intelligence to interpret, generalize, and harness this data for sustainable and predictive engineering solutions.

As mentioned, DIC represents an optical measurement technique that operates without physical contact, utilizing image analysis to obtain comprehensive field data regarding deformation and strain across various scales [19].

Through the implementation of image registration algorithms, this methodology is adept at determining the relative displacements of material points between a reference image (commonly representing the undeformed state) and a current image (typically depicting the deformed state) [20, 21], a process necessitated by the dissimilar dot patterns observed in the current image in comparison to the initial reference image.

In spite of multiple proposed enhancements to the fundamental computational algorithms, Blaber et al. [22] have created an open-source, readily accessible two-dimensional subset-based digital image correlation software suite (Ncorr) that integrates contemporary algorithms articulated in scholarly discourse, alongside numerous supplementary refinements and modifications aimed at addressing deficiencies such as the absence of a modern, adaptable, and user-friendly code. In Ncorr, the subsets are initially defined as a contiguous circular aggregation of points situated at integer pixel locations within the reference configuration, which serves to mitigate computational expenses, while the deformation is presupposed to be uniform within each subset.

In Fig. 1, an example of a set of selected points and their corresponding coordinates in the reference image and the secondary state image can be seen [22].

According to Fig. 1, an (i,j) coordinate is assigned to each point under examination. All new (i,j) coordinates can be calculated using Eq. (1).

$$X_{curi}=X_{refi}+u_{rc}+\partial u/\partial X_{rc}(X_{refi}-X_{refc})+ +\partial u/\partial Y_{rc}(Y_{refj}-Y_{refc})$$
$$Y_{curj}=Y_{refj}+v_{rc}+\partial v/\partial Y_{rc}(X_{refi}-X_{refc})+ +\partial v/\partial Y_{rc}(Y_{refj}-Y_{refc}) \quad (1)$$

In this context, x_{refi} and y_{refj} denote the x and y coordinates of a designated point within the initial reference subset, x_{refc} and y_{refc} represent the

coordinates of the centroid of the initial reference subset, and X_{curi} and Y_{curj} indicate the coordinates of a point within the current subset. The subscript "rc" employed in eq. 1 is intended to denote the transformation from the reference coordinate system to the current coordinate system.

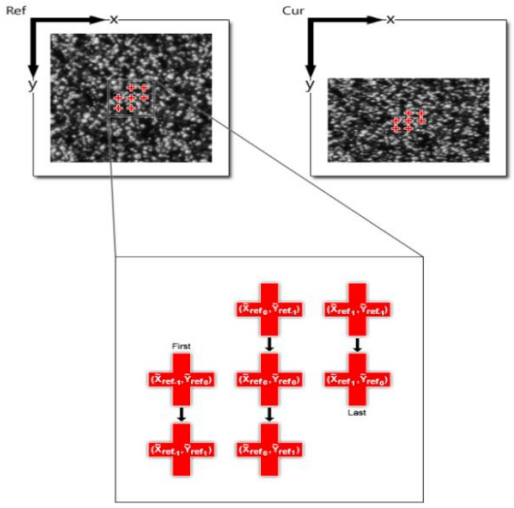

Fig. 1. The subset's coordinates [22].

The deformation is characterized by displacements u and v along with their derivatives, all of which remain constant for a specified subset. Eq. 2 articulates a generalized deformation vector P. The indices (i,j) serve to denote the relative positioning of the points in relation to the center of the subset, as well as to facilitate correspondences between subset points in both the current and reference configurations, while P denotes a collection that encompasses all of the subset points.

$$P = \{u \quad v \quad \partial u/\partial x \quad \partial u/\partial y \quad \partial v/\partial x \quad \partial v/\partial y\}^T \qquad (2)$$

The overall deformation occurring on the surface where the points are tracked during DIC is shown in Fig. 2.

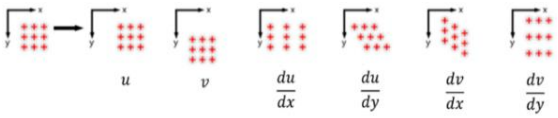

Fig. 2. Linear transformations for subset coordinates [22].

The difference in background and point colors creates a matrix of black and white color coefficients. This matrix is unique to each point with its specific color code, allowing the tracking of that code throughout the experiment. In Fig. 3, the assignment of black and white color coefficient codes for each tracked point is displayed.

In this figure, the closer the displacement of the tracked point on the surface approaches zero, the darker (black) its color becomes; conversely, the closer the displacement approaches one, the color of the corresponding point becomes closer to white. For more detailed information on the algorithms used in the software, the reader is referred to [22].

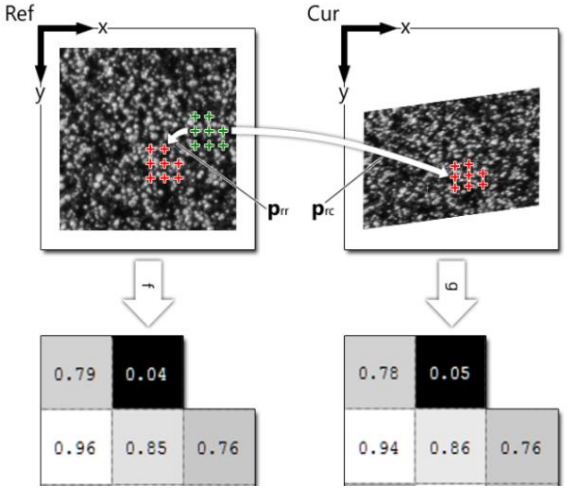

Fig. 3. Grayscale values in the reference and current configuration [22].

A resistive strain gauge can be described as a thin strip of metal that is specifically engineered with the purpose of accurately measuring mechanical load by exhibiting a change in electrical resistance in response to the application of stress [23]. Given the typical range of resistance variation that is observed in strain gauges, it becomes essential that in order to effectively utilize the strain gauge as a reliable and functional instrument, one must be capable of detecting and measuring extremely minute changes in resistance with a high level of precision. Such meticulous and exacting requirements for precision in measurements necessitate the utilization of a Wheatstone bridge measurement circuit.

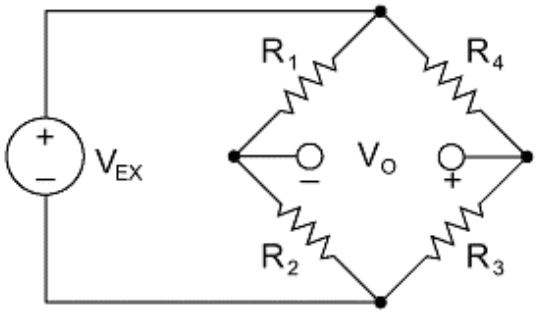

Fig. 4. Full Wheatstone bridge circuit configuration.

Fig. 4 illustrates the comprehensive circuit configuration of the Wheatstone bridge that is employed in the present study, wherein R_1, R_2, R_3, and R_4 denote the various electrical resistances

present in the circuit, while V_E and V_o represent the supply voltage and the output voltage, respectively, that characterize the operational parameters of the circuit [23]. The mathematical representation of the full Wheatstone bridge circuit can be found in the form of Eq. (3).

$$V_o=V_{EX}(R_3/(R_3+R_4)-R_2/(R_1+R_2)) \quad (3)$$

The utilization of DIC has also been expanded significantly across other domains, including the exploration of DIC's efficacy in quantifying full-field strain in timber materials [24], cementitious materials [25], brick masonry specimens [26], axially loaded collateral ligaments [27], and elastomeric materials [28].

Some researchers also have paid attention to study and compare the potential of the DIC against resistive strain gauge method [28, 29].

Casita et al. [30] conducted an investigation into the stress-strain response of tensile steel specimens with varying thicknesses through two methodologies: DIC and the traditional experimental uniaxial tensile test. The findings revealed that both methodologies yielded comparable values for tensile strength and Young's modulus. Nonetheless, the DIC methodology yielded marginally lower values than the conventional approach, yet it was still deemed precise for the prediction of tensile properties.

Grytten et al. [31] undertook an experimental assessment of the mechanical behavior exhibited by a talc and elastomer-modified polypropylene compound when subjected to substantial strains through the application of two distinct methodologies: DIC and stereo-vision.

The tensile properties of an array of materials, specifically aluminum A1100, glass fiber-reinforced plastics, and pure resin plastics, were explored utilizing experimental techniques, strain gauge measurements, and DIC methodologies. It was determined that the three methodologies rendered closely aligned values for Young's modulus, with the tensile specimen composed of aluminum exhibiting the highest value in comparison to the other two materials. Furthermore, it was emphasized that the DIC methodology produced a marginally higher value than the experimental technique [32]. The DIC methodology was effectively employed in a mini-tensile apparatus for the mechanical characterization of sheet metal by Cruz et al. [33].

Based on a literature review, it is observed that the potential of DIC method compared to other techniques, particularly resistive strain gauges, has been a focus of many researchers. In line with this, the present study investigates the stress-strain behavior of a steel specimen under tensile loading using two methods: DIC and resistive strain gauges, to calculate the modulus of elasticity. This approach can be generalized to other components and engineering applications such as sustainable energy systems where installing strain gauges is limited or analytical relations are unavailable.

2. Experimental set up and specimen preparation

To compare the capabilities of the DIC and resistive strain gauge methods, a steel tensile test specimen subjected to loading by a tensile testing machine is used. The tensile testing procedure is performed utilizing a standard universal testing apparatus, specifically the Santam Company model AST-250, which possesses a maximum load capacity of 250 kN.

Two specimen are used in the present work. The first specimen is made of ST52 steel, with an elastic modulus of 210 GPa and the second specimen made of ST37 steel, with an elastic modulus of 195 GPa [34]. A uniaxial resistive strain gauge model BHF350-10AA (350±0.3% ohms, gauge factor 2.1±1%) is installed along the length of one side of the specimen. The opposite side is prepared for DIC by applying white spray paint and titanium dioxide powder (see Fig. 5(b)).

Image sequences for DIC analysis are extracted from a 4K resolution video (3840×2160 pixels) recorded at a frame rate of 24 frames per second. This video encapsulates the entire loading procedure, and specific frames indicative of pivotal moments of force application are subsequently selected for analytical processing. The camera is strategically positioned 35 cm away from the specimen of the tensile testing apparatus, ensuring parallel alignment with both the device and the specimen facilitated by a digital leveling instrument.

Digital image analysis is conducted utilizing the Ncorr algorithm [19] within the MATLAB software environment. The subset size must encompass a sufficient array of distinct features to achieve a robust correlation. Additionally, it has been observed that smaller subset radii are more susceptible to the noise inherent in each simulated image [22]. Accordingly, a subset radius of 86 pixels and a subset spacing of 9 pixels are deemed appropriate for this analysis.

Speckles are generated through the application of titanium dioxide combined with 99% pure isopropyl alcohol. The mixture of these two substances is maintained at an approximate ratio of 10%, after which it is applied to the surface via manual spraying techniques. It is worth noting that

applying a pure axial force and ensuring the camera is perpendicular to the specimen surface enhances the accuracy of the results.

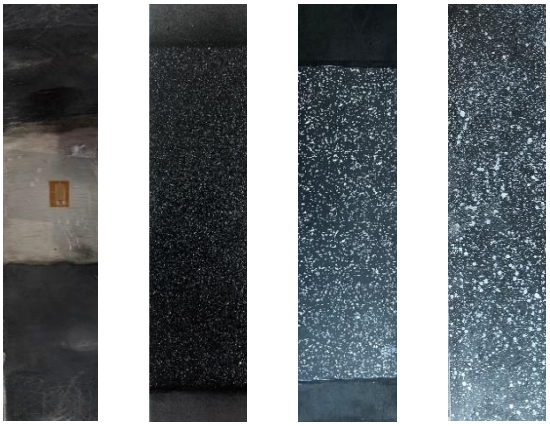

Fig. 5. The prepared specimen: a) The installed strain gauge; b) Prepared using spray paint; c) Prepared using titanium dioxide; d) Prepared using large size speckles.

According to Fig. 5, the specimen has a black background color with very small white spots on it (Fig. 5(b)). In this state, the contrast between the background color and the spots reaches its maximum, making pixel tracking easier. Both resistive strain gauging and DIC are symmetrically performed on both sides of the specimen, and the strain measurement results are recorded simultaneously. Due to the application of a pure axial force, the stress resulting from the tensile force is given by Eq. (4).

$$\sigma=F/A \quad (4)$$

Here, F is the applied force and A is the cross-sectional area of the specimen. The specimen under test is loaded within the elastic range, so the relationship between stress and strain can be expressed using Hooke's law ($\sigma=E\varepsilon$), where E is the elastic modulus.

3. Results and discussion

After preparing the specimen, the tension device was adjusted to gradually increase the applied tensile force in 11 steps from 2,500 N to 27,500 N, while strain values from both methods were recorded simultaneously. Fig. 6 illustrates the experimental setup of the tensile test. The Region of interest is delineated based on the area encompassing the gauge and the strain field that is to be assessed.

Each experimental condition is repeated three times and the average value is reported finally. Various stress values along with strain values obtained from the analytical and the resistive strain gauge methods are presented in Fig. 7.

Fig. 6. Experimental setup.

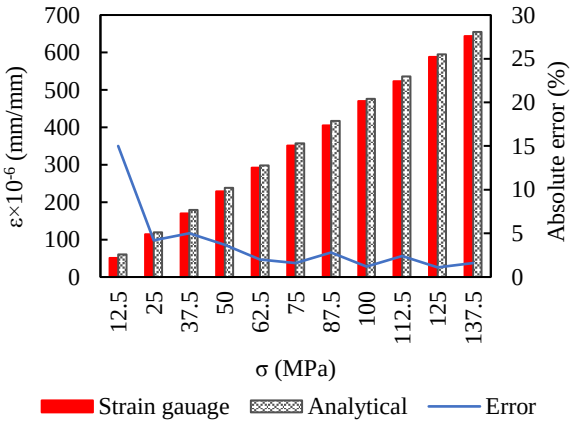

Fig. 7. Comparison of the strain measurements through analytical and resistive strain gauge methods.

The average absolute error of approximately 3.7% in strain values measured by the resistive strain gauge method compared to the analytical method indicates the accuracy of the extracted results and the capability of this method to measure strain values. Furthermore, it is evident that the accuracy of the measurements obtained by this method improves as the applied force (and consequently, the resulting strain) increases. Specifically, the absolute error decreases from 15% at an applied stress of 12.5 MPa to about 1.5% at an applied stress of 137.5 MPa.

Strain variations with respect to applied stress for the DIC method compared to the other two methods are also shown in Fig. 8. It can be observed that the DIC method is quite capable of predicting the linear behavior between stress and strain in the tested specimen. The correlation coefficient (R^2) of 0.9549 for this method, compared to values close to 1 for both the analytical method and the use of strain gauge,

highlights this point. The DIC method reports the elastic modulus of the steel specimen to be about 116 GPa, which, compared to values of 210 obtained from the analytical method and 211 GPa (standard deviation of 2.49 GPa and standard error of 1.44 GPa) resulted from the strain gauge method, indicates an error of approximately 45%.

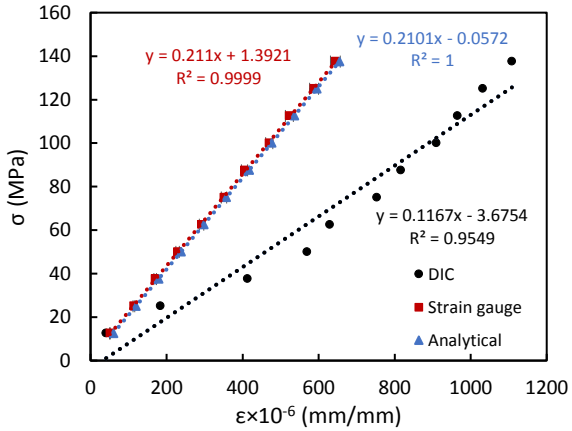

Fig. 8. Comparison of the stress-strain plots for DIC, analytical and resistive strain gauge methods (specimen prepared using white paint spray).

It should be mentioned that, the above various reported values of the elastic modulus come from different applied methods (DIC method, analytical method and strain gauge method). This calculated error suggests that despite the high capability of this method in predicting the linear relationship between stress and strain, its results lack high accuracy. Furthermore, the results show that the DIC method has greater accuracy in predicting strain values at lower applied stress levels, while the error increases as the applied stress increases. The increased deviation of the DIC method at higher applied forces can be attributed to various factors, including loss of the tracked point during the tracking process due to excessively small speckles, low color contrast between speckles and the background, and low quality of the imaging camera. In fact, improving camera quality allows for a higher number of recorded pixels and consequently greater accuracy in results. To address these issues, specific solutions are recommended, such as using chemical agents to enhance the brightness of the speckles and create sharper edges between the background and the colored speckles, as well as increasing the speckle size to cover more pixels and improve the ability to track them. Considering the above points, the second specimen made of ST37 steel, with an elastic modulus of 195 GPa [34], is prepared using titanium dioxide powder (Fig. 5 (c)) and subjected to loading. This powder is more reflective than paint and, due to its powder form, creates very sharp, shadow-free speckle edges, which enhances the accuracy of image processing. The stress-strain curve obtained using the DIC method with titanium dioxide powder, compared to the other two methods, is plotted in Fig. 9.

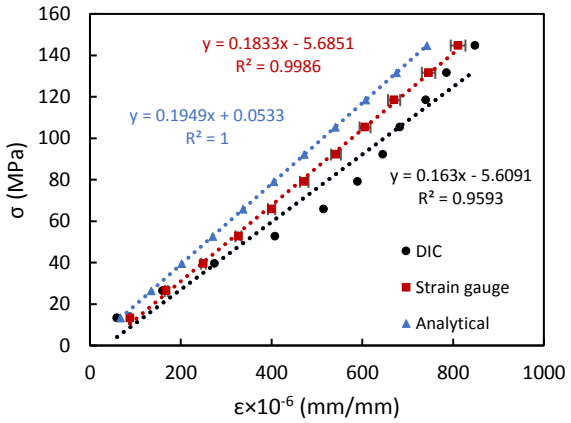

Fig. 9. Comparison of the stress-strain plots for DIC, analytical and resistive strain gauge methods (specimen prepared using titanium dioxide).

It is observed that by using titanium dioxide powder, the error of the DIC method in predicting the modulus of elasticity has significantly decreased. In fact, the error value is decreased from 45% compared to the analytical method results to about 15%, which is acceptable in engineering calculations. It should be mentioned that the reported value of the elastic modulus is 183 GPa with the standard deviation of 1.7 GPa and standard error of 0.98 GPa.

Despite the acceptable error in predicting results using titanium dioxide powder, it will still be possible to reduce the error of the image processing method by using a higher quality camera and also by changing the dimension of the speckles used for tracking.

Next, to investigate the effects of speckle size on the results obtained from the DIC method, the size of the colored speckles on the specimen is increased (Fig. 5 (d)), and reloading is performed. It is observed that using titanium dioxide powder with larger speckle sizes, results in elastic modulus of 184 GPa with the standard deviation of 2.35 GPa and standard error of 1.36 GPa which shows that the error of the DIC method in predicting the modulus of elasticity is significantly decreased. In fact, the error value is decreased from 15% compared to the analytical method results to about 6%, which is completely acceptable and indicates the high potential of the proposed method (Fig. 10). A sensitivity analysis is regarded as a methodological approach to assess the significance

of each input parameter on the corresponding output parameters.

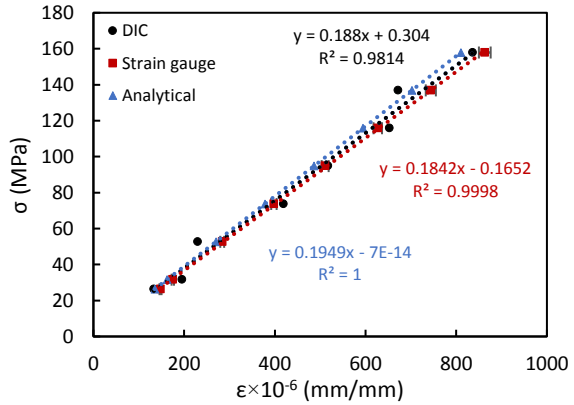

Fig. 10. Comparison of the stress-strain plots for DIC, analytical and resistive strain gauge methods (specimen prepared using large size speckles).

This type of analysis elucidates which input parameters exhibit the greatest and least significance during the modeling process. The contribution of each input to various outputs can be ascertained by systematically varying the specified input while maintaining other inputs at constant levels. When considering the subset radius, step spacing, and strain radius as input parameters, and the elastic modulus as the output parameter, it is evident that the subset radius and step spacing exhibit sensitivities of 0.053 and 0.15, respectively, whereas the dependence on variations in the strain radius is minimal. This analysis underscores that the output parameter demonstrates the highest sensitivity to changes in step spacing.

5 kN

6 kN

10 kN

14 kN

18 kN

22 kN

26 kN

30 kN

Fig. 11. Image of DIC method under applied loads.

The contour plot images obtained from the DIC Ncorr software are portrayed in Fig. 11. This figure provides the contour plot of measured displacements under varying applied loads. The figure clearly shows that increasing the applied load results in displacement increment, in which the color varies in an extensive range (approximately from blue to red).

Based on the demonstrated capabilities of the DIC methodology, it can be regarded as a highly accurate and versatile instrument for full-field displacement and strain measurement across diverse domains. Renewable energy systems are dependent on mechanical components (such as turbine blades, towers, and support frameworks) that are continually subjected to dynamic loads, fatigue, and environmental influences. The DIC technique, characterized by its non-contact, full-field, optical-based, and non-destructive testing approach, provides a formidable means of monitoring deformation and strain within these components. For instance, due to the heterogeneous or composite nature of the blade, which is affected by nonlinear or fatigue characteristics, the strain distribution on the surface can reveal critical locations. Employing the DIC method enables the identification and optimization of these critical points. Recently, this methodology has been integrated into machine learning and artificial intelligence; the amalgamation of DIC with AI transforms traditional experimental observations into intelligent diagnostic frameworks capable of real-time structural evaluation and automated decision-making. This confluence not only expedites the interpretation of data but also facilitates the advancement towards self-learning, adaptive systems in the fields of material and structural engineering.

4. Conclusion

Given the increasing need for strain measurement in various industries to examine stress and strain distribution in mechanical parts and identify critical points, novel methods such as DIC have gained widespread attention in recent years. Non-contact nature, lower cost, and higher speed can be considered as features of this method. In this research, the capability of strain measurement by the DIC method was investigated in comparison with the analytical method and also the conventional method of using resistance strain gauges for measuring the strain of a tensile steel specimen under tensile force, and the obtained results were used to calculate the modulus of elasticity. When using spray paint for specimen preparation, an error of 45% was observed in predicting the modulus of elasticity compared to the resistance strain gauge and analytical methods. It was suggested that to increase the accuracy of the results obtained from the DIC method, titanium dioxide powder should be used for specimen preparation to increase the brightness of the spots and create sharper edges between the background and the created colored spots, which resulted in an approximately 35% reduction in the error of predicting the modulus of elasticity compared to the resistance strain gauge method. Also, the use of a higher quality camera and changing the size of the spots used for tracking were suggested, and the use of larger speckles reduced the error in predicting the modulus of elasticity to less than 5% compared to the other methods.

Acknowledgements

The authors sincerely thank Mr. Abbas Bahrami Vahdat, the esteemed CEO of Moien Industrial Group, for his efforts and support in providing laboratory supplies and equipment for this research.

References

[1] Meng, W., Bachilo, S. M., Weisman, R. B., & Nagarajaiah, S. (2024). A Review: Non-Contact and Full-Field Strain Mapping Methods for Experimental Mechanics and Structural Health Monitoring. *Sensors*, *24*(20), 6573.

[2] Sutton, M. A., Wolters, W. J., Peters, W. H., Ranson, W. F., & McNeill, S. R. (1983). Determination of displacements using an improved digital correlation method. *Image and vision computing*, *1*(3), 133-139.

[3] Peters, W. H., & Ranson, W. F. (1982). Digital imaging techniques in experimental stress analysis. *Optical engineering*, *21*(3), 427-431.

[4] Barone, S., Neri, P., Paoli, A., & Razionale, A. V. (2019). Low-frame-rate single camera system for 3D full-field high-frequency vibration

measurements. *Mechanical Systems and Signal Processing*, *123*, 143-152.

[5] Poozesh, P., Sabato, A., Sarrafi, A., Niezrecki, C., Avitabile, P., & Yarala, R. (2020). Multicamera measurement system to evaluate the dynamic response of utility-scale wind turbine blades. *Wind Energy*, *23*(7), 1619-1639.

[6] Yang, J., Peng, C., Xiao, J., Zeng, J., & Yuan, Y. (2012). Application of videometric technique to deformation measurement for large-scale composite wind turbine blade. *Applied Energy*, *98*, 292-300.

[7] Feng, W., Yang, D., Du, W., & Li, Q. (2023). In situ structural health monitoring of full-scale wind turbine blades in operation based on stereo digital image correlation. *Sustainability*, *15*(18), 13783.

[8] Ha, K., Kang, M., Kwon, D., Hwang, S., & Yoo, C. (2024). Application of 3D Digital Image Correlation Technique to Measurement of Wind Blade Properties from Coupon Test and Small-Sized-Blade Frequency Test. *Energies*, *17*(4), 909.

[9] Langston1a, D., Mahadik, Y., Greaves, P., Thomsen, O., & Macquart, T. Application of Digital Image Correlation (DIC) to torsional tests of a 40m wind turbine blade.

[10] Lehnhoff, S., Gómez González, A., & Seume, J. R. (2020). Full scale deformation measurements of a wind turbine rotor in comparison with aeroelastic simulations. *Wind Energy Science Discussions*, *2020*, 1-18.

[11] Winstroth, J., & Seume, J. R. (2014). Wind turbine rotor blade monitoring using digital image correlation: 3d simulation of the experimental setup. *European Wind Energy Association-EWEA*.

[12] Abdelsattar, M., AbdelMoety, A., & Emad-Eldeen, A. (2025). ResNet-based image processing approach for precise detection of cracks in photovoltaic panels. *Scientific Reports*, *15*(1), 24356.

[13] Rahman, A. (2025). Solar Panel Surface Defect and Dust Detection: Deep Learning Approach. *Journal of Imaging*, *11*(9), 287.

[14] Scenini, F., Azough, F., Read-Jennings, M. C., & Shoesmith, J. P. (2012, May). Use of Digital Image Correlation (DIC) for detection of defects and monitoring of structural integrity in the nuclear industry. In *9th International Conference on NDE in Relation to Structural Integrity for Nuclear and Pressurized Components*.

[15] Shirazi, H., Wang, S., Eadie, R., & Chen, W. (2024). Pipeline Circumferential Cracking in Near-Neutral pH Environment Under the Influence of Residual Stress: Dormancy and Crack Initiation. *Metallurgical and Materials Transactions A*, *55*(9), 3640-3661.

[16] Yang, R., Li, Y., Zeng, D., & Guo, P. (2022). Deep DIC: Deep learning-based digital image correlation for end-to-end displacement and strain measurement. *Journal of Materials Processing Technology*, *302*, 117474.

[17] Melching, D., Strohmann, T., Requena, G., & Breitbarth, E. (2022). Explainable machine learning for precise fatigue crack tip detection. *Scientific reports*, *12*(1), 9513.

[18] Boukhtache, S., Abdelouahab, K., Berry, F., Blaysat, B., Grediac, M., & Sur, F. (2021). When deep learning meets digital image correlation. *Optics and Lasers in Engineering*, *136*, 106308.

[19] Pan, B., Qian, K., Xie, H., & Asundi, A. (2009). Two-dimensional digital image correlation for in-plane displacement and strain measurement: a review. *Measurement science and technology*, *20*(6), 062001.

[20] Bruck, H. A., McNeill, S. R., Sutton, M. A., & Peters Iii, W. H. (1989). Digital image correlation using Newton-Raphson method of partial differential correction. *Experimental mechanics*, *29*(3), 261-267.

[21] Cheng, P., Sutton, M. A., Schreier, H. W., & McNeill, S. R. (2002). Full-field speckle pattern image correlation with B-spline deformation function. *Experimental mechanics*, *42*(3), 344-352.

[22] Blaber, J., Adair, B., & Antoniou, A. (2015). Ncorr: open-source 2D digital image correlation matlab software. *Experimental Mechanics*, *55*(6), 1105-1122.

[23] Sharpe Jr, W. N., & Sharpe, W. N. (Eds.). (2008). *Springer handbook of experimental solid mechanics*. Springer Science & Business Media.

[24] Melinda, A. P., Yoresta, F. S., Higuchi, S., Yamazaki, Y., & Matsumoto, Y. (2023). Investigation of the accuracy of Digital Image Correlation (DIC) in measuring full-field strain for timber materials. In *E3S Web of Conferences* (Vol. 464, p. 09002). EDP Sciences.

[25] Tambusay, A., Suryanto, B., & Suprobo, P. (2020). Digital image correlation for cement-based materials and structural concrete testing. *Civil Engineering Dimension*, *22*(1).

[26] Kumar, S. L., Aravind, H. B., & Hossiney, N. (2019). Digital image correlation (DIC) for measuring strain in brick masonry specimen using Ncorr open source 2D MATLAB program. *Results in Engineering*, *4*, 100061.

[27] Prusa, G., Bauer, L., Santos, I., Thorwächter, C., Woiczinski, M., & Kistler, M. (2023). Strain evaluation of axially loaded collateral ligaments: a comparison of digital image correlation and strain gauges. *BioMedical Engineering OnLine*, *22*(1), 13.

[28] Ramos, T., Braga, D. F., Eslami, S., Tavares, P. J., & Moreira, P. M. G. P. (2015). Comparison between finite element method simulation, digital image correlation and strain gauges measurements in a 3-point bending flexural test. *Procedia Engineering*, *114*, 232-239.

[29] Huang, Y. H., Liu, L., Sham, F. C., Chan, Y. S., & Ng, S. P. (2010). Optical strain gauge vs. traditional strain gauges for concrete elasticity modulus determination. *Optik*, *121*(18), 1635-1641.

[30] Casita, C. B., Iranata, D., Suswanto, B., &

Matsumura, M. (2024). Graphical Representation of Uniaxial Tensile Test Through Digital Image Correlation. *Geomate Journal*, *27*(122), 28-35.

[31] Grytten, F., Daiyan, H., Polanco-Loria, M., & Dumoulin, S. (2009). Use of digital image correlation to measure large-strain tensile properties of ductile thermoplastics. *Polymer Testing*, *28*(6), 653-660.

[32] Quanjin, M., Rejab, M. R. M., Halim, Q., Merzuki, M. N. M., & Darus, M. A. H. (2020). Experimental investigation of the tensile test using digital image correlation (DIC) method. *Materials Today: Proceedings*, *27*, 757-763,

[33] Cruz, D. J., Shamchi, S. P., Santos, A. D., Amaral, R. L., Tavares, P. J., & Moreira, P. M. G. P. (2020). Development of a mini-tensile approach for sheet metal testing using Digital Image Correlation. *Procedia Structural Integrity*, *25*, 316-323.

[34] Davis, J. R. (1996). *ASM specialty handbook-carbon and alloy steels*. ASM International, Materials Park, Ohio.

Biography

Amir Masoud Hamidi Majd holds a M.Sc. degree in Mechanical Engineering from Shahid Beheshti University, Tehran, Iran. His research interests include instrumentation, measurement systems, and image processing, with an emphasis on experimental methodologies and data-driven approaches in mechanical engineering.

Dr. Seyed Ebrahim Mousavi Torshizi is a faculty member of the Department of Mechanical Engineering at Shahid Beheshti University, Tehran, Iran. He holds a Ph.D. in Mechanical Engineering and has extensive experience in teaching, research, and industrial collaboration. His research interests include failure analysis of mechanical and power plant components, mechanical behavior of materials under fatigue and creep conditions, and experimental stress analysis. He has been involved in numerous applied research projects in the energy and power generation sectors and has published widely in peer-reviewed international journals.

Javad Zare graduated in Mechanical Engineering from Iran University of Science and Technology, Tehran, Iran. His research focuses on thermal-fluid sciences and energy systems. Specific interests include computational fluid dynamics (CFD), heat exchanger modeling and optimization, refrigeration systems, and nanofluidics. His work also encompasses fundamental principles of heat transfer and thermodynamics as they apply to advanced energy systems and renewable energy technologies.